Calculating free energies for diffusion in tight-fitting zeolite-guest systems: Local normal-mode Monte Carlo

Srinivas C. Turaga
Department of Chemistry and Department of Computer Science, University of Massachusetts, Amherst, Massachusetts 01003

Scott M. Auerbach[a)]
Department of Chemistry and Department of Chemical Engineering, University of Massachusetts, Amherst, Massachusetts 01003

(Received 27 November 2002; accepted 13 January 2003)

We present an efficient Monte Carlo algorithm for simulating diffusion in tight-fitting host–guest systems, based on using zeolite normal modes. Computational efficiency is gained by sampling framework distortions using normal-mode coordinates, and by exploiting the fact that zeolite distortion energies are well approximated by harmonic estimates. Additional savings are obtained by performing local normal-mode analysis, i.e., only including the motions of zeolite atoms close to the jumping molecule, hence focusing the calculation on zeolite distortions relevant to guest diffusion. We performed normal-mode analysis on various silicalite structures to demonstrate the accuracy of the harmonic approximation. We computed free energy surfaces for benzene in silicalite, finding excellent agreement with previous theoretical studies. Our method is found to be orders-of-magnitude faster than comparable Monte Carlo calculations that use conventional forcefields to quantify zeolite distortion energies. For tight-fitting guests, the efficiency of our new method allows flexible-lattice simulations to converge in less CPU time than that required for fixed-lattice simulations, because of the increased likelihood of jumping through a flexible lattice. [DOI: 10.1063/1.1558033]

I. INTRODUCTION

The transport properties of adsorbed molecules play a central role in determining selectivities of reactions and separations in zeolites, especially when adsorbate sizes approach zeolite pore dimensions.[1,2] In particular, the tight fit of C_6–C_8 aromatics in MFI-type zeolites (see Fig. 1) produces a variety of interesting effects that signal the importance of zeolite framework flexibility. These include framework phase transitions induced by guest adsorption,[3–5] and anomalously high fluxes of ortho-xylene through zeolite membranes with co-adsorbed para-xylene.[6,7] Computational studies have the potential to shed light on these intriguing phenomena, by elucidating the coupling between guest motion and zeolite distortion. However, flexible-lattice simulations on tight-fitting systems are rare because they are computationally demanding, even when exploiting methods specialized for infrequent events.[8] In this article, we develop an efficient Monte Carlo algorithm for simulating diffusion in tight-fitting host–guest systems, based on using zeolite normal modes.

Systematic comparisons of fixed- and flexible-lattice molecular dynamics (MD) simulations have been reported for a variety of *loose-fitting* zeolite-guest systems, including methane and light hydrocarbons in silicalite,[9–13] methane in cation-free LTA,[14] Lennard-Jones adsorbates in Na-A[15] and in Na-Y,[16] benzene and propylene in MCM-22,[17] benzene in Na-Y,[18–20] and methane in $AlPO_4$-5.[21] It is not surprising that for these relatively small guests, lattice flexibility does not influence diffusion. Studies on tighter-fitting systems, such as benzene and propene in MCM-22,[17] and iso-butane[13] and benzene[8,22] in silicalite, do indeed show that lattice flexibility strongly influences diffusion. In particular, Snurr *et al.* applied harmonic transition state theory (TST) to benzene diffusion in silicalite, assuming that benzene and silicalite remain rigid.[22] As a consequence of this assumption, their results underestimate experimental diffusivities by one to two orders of magnitude. Forester and Smith subsequently applied TST to benzene in silicalite using constrained reaction-coordinate dynamics on both rigid and flexible lattices.[8] Lattice flexibility was found to have a very strong influence on the jump rates. Diffusivities obtained from these flexible framework simulations are in excellent agreement with experiment, overestimating the measured room temperature diffusivity (2.2×10^{-14} $m^2\,s^{-1}$) by only about 50%. These studies establish benzene in silicalite as an important benchmark system for which including framework flexibility is crucial for describing guest diffusion.

Despite the importance of modeling diffusion in tight-fitting zeolite–guest systems, such calculations are rare because they are so challenging. To remedy this situation, an efficient approach will have to (i) reduce the added expense of calculating framework distortion energies, and (ii) sample cooperative motions of the zeolite, because these are likely to facilitate guest diffusion. The constrained reaction-coordinate dynamics reported by Forester and Smith do indeed produce cooperative zeolite motions. However, this is

a)Author to whom correspondence should be addressed. Electronic mail: auerbach@chem.umass.edu

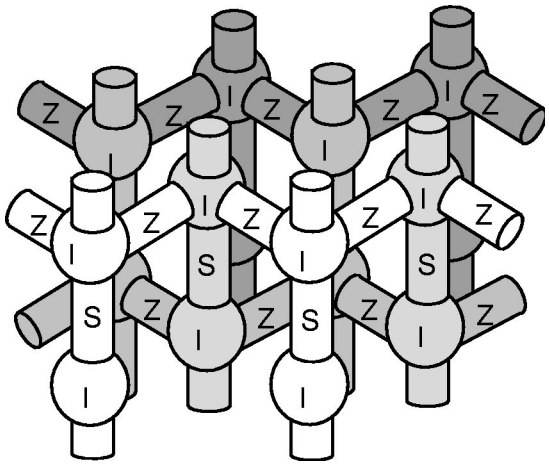

FIG. 1. MFI zeolite topology: S/Z are Straight/Zig–zag channels; I is Intersection.

achieved at significantly greater computational expense than that of fixed-lattice simulations.

A solution satisfying both criteria is suggested by the normal-mode analyses of zeolite vibrations reported by Iyer and Singer.[23] They found that zeolite normal modes often correspond to breathing motions of rings and channels, suggesting that these coordinates can efficiently sample framework distortions during molecular jumps. What's more, a remarkable speedup can be obtained by exploiting the fact that zeolite vibrations are nearly harmonic, which we show below. As such, after computing the normal modes, sampling lattice flexibility costs *essentially no CPU time* because the zeolite force constants are known. Thus, we use normal-mode coordinates for natural sampling of zeolite vibrations, and normal-mode force constants for efficient energy calculations. Below we calculate free energy surfaces for benzene jumping in silicalite's straight channel (see Fig. 1), finding excellent agreement with the results of Forester and Smith.[8] However, in contrast with their calculations, the flexible-lattice simulations reported below converged in *less CPU time* than that required for fixed-lattice simulations.

The remainder of this article is organized as follows: Section II outlines the local normal-mode algorithm, in addition to the forcefields and free energy methods we utilize. Section III provides results and discussion of normal-mode analyses and free energy surfaces, and Sec. IV offers a summary of our findings as well as concluding remarks.

II. METHODS

We calculate free energy surfaces (FES) for benzene to move along silicalite's straight channel from one intersection site to the next, using the *y*-component of benzene's center-of-mass as a reaction coordinate. The FES is formally defined by

$$F(y_0) \equiv -k_B T \ln[L\langle \delta(y-y_0)\rangle_T], \tag{1}$$

where k_B is Boltzmann's constant, T is temperature, $\langle \cdots \rangle_T$ is a canonical average, $\delta(y-y_0)$ is Dirac's delta function, and L is a formal length scale that cancels when computing free energy differences. Here we discuss the base model and forcefield, the free energy sampling method, and last but not least, the local normal-mode algorithm.

A. Base model and forcefield

As with our previous simulations of benzene in silicalite,[24,25] the simulation cell we adopt consists of two silicalite unit cells along the *z*-axis,[26] containing a total of 192 silicons and 384 oxygens under three-dimensional periodic boundary conditions. As such, our simulation cell has the dimensions 20.02 Å$\times$19.90 Å $\times$26.77 Å. We add to this model of bulk silicalite one benzene molecule; all 588 particles interact via Coulombic and short-ranged forces. Coulombic energies are calculated with Ewald summations, and short-ranged forces are cut-and-shifted at 9.9 Å. We utilize the framework forcefield developed by us for modeling alumino-silicates,[27] which has also been applied to siliceous materials as well.[24,25] We adopt the zeolite–benzene interaction potential reported in our initial work on benzene in Na-Y.[28] For computational simplicity we fix benzene's internal coordinates. This approximation is expected to be a good one, because the relative rigidity of benzene compared to that of the zeolite makes it unlikely that internal vibrations of benzene facilitate its diffusion. For future work, we will relax this constraint by considering harmonic guest vibrations alongside harmonic zeolite distortions.

B. Free energy surface calculations

We partition three-dimensional space in silicalite's straight channel by defining a sequence of planes perpendicular to the jump coordinate, *y*, from one intersection site to the next. Adjacent planes are typically separated by 0.4 Å; this distance is chosen to minimize the number of planes (and hence free energy calculations) while maximizing the overlap between adjacent potential energy distributions. The difference between free energies in adjacent regions A and B is given by: $\Delta F = F_B - F_A = -k_B T \ln(Q_B/Q_A)$, where Q_i is the canonical partition function in region i=A or B. We calculate the ratio of partition functions using Voter's displacement-vector method.[29,30] In this approach, the ratio of partition functions is computed using two Monte Carlo averages as follows:

$$\frac{Q_B}{Q_A} = \frac{\langle M_\beta[V_B(\mathbf{r}+\mathbf{d}) - V_A(\mathbf{r})]\rangle_A}{\langle M_\beta[V_A(\mathbf{r}-\mathbf{d}) - V_B(\mathbf{r})]\rangle_B}. \tag{2}$$

In Eq. (2), the numerator is the average probability of making a jump from point $\mathbf{r}$ in region A to point $\mathbf{r}+\mathbf{d}$ in region B, via the displacement vector $\mathbf{d}$. This jump involves both translational and rotational motion, the latter generated by random changes in benzene's Euler angles. The subscript ''A'' on the average in the numerator reminds us that these jumps from A to B are fictitious, i.e., they are never actually accepted during the sampling of region A. However, the acceptance statistics are accumulated in the numerator. The denominator is the probability of going in the opposite direction, from region B to A, via the displacement vector $-\mathbf{d}$. For the denominator, statistics for fictitious jumps are accumulated during a standard canonical sampling of region B.

To hasten convergence, we choose displacement vectors randomly from a Gaussian distribution centered on $\mathbf{d}_0 = (0, 0.4, 0)$ Å, with Cartesian widths of (0.2, 0.2, 0.2) Å; these widths were chosen to optimize the sampling of jumps. Because of the dispersion in the *y*-component of the displacement vector, jumps outside the target region are occasionally produced. These are wrapped back into the target region by adding or subtracting $\mathbf{d}_0$ as appropriate. This procedure introduces no bias into the generation of jumps. In all cases, the Monte Carlo acceptance probability is modeled using the Metropolis function $M_\beta(\Delta E) = \min[1, \exp(-\beta \Delta E)]$, which depends on the difference in potential energy between the points in the two regions. The energies required for this calculation are evaluated using the local normal-mode scheme, which we now describe.

C. Normal mode Monte Carlo

Here we describe the generation of normal modes, the use of normal-mode coordinates for updating zeolite configurations, and the use of normal-mode force constants for calculating zeolite distortion energies. We begin by choosing the zeolite atoms allowed to move. This choice depends upon the problem at hand, in particular the host, guest and jump under consideration. For the model of silicalite we consider here, the number of movable zeolite atoms (N) satisfies $N \leqslant 576$. When performing normal-mode analysis to test the harmonic approximation, we use $N = 576$. On the other hand, when computing the FES, we generally use $N < 576$.

For the intersection → straight channel → intersection jump of benzene in silicalite, we used a cylindrical cut-off to choose movable zeolite atoms. The cylindrical radius is subject to optimization: too small a radius includes too few atoms, leaving the channel too rigid and the method inaccurate; while too large a radius produces too many irrelevant normal modes, leaving the method inefficient. Although in principle one should explicitly converge a FES with respect to the cut-off radius, in practice such explicit convergence is computationally demanding. Instead, we increase the radius and look for convergence in the distribution of normal-mode force constants (data not shown). When gauging convergence, we ignore the low-frequency Debye region ($\bar{\nu} \lesssim 80$ cm^{-1}; see Fig. 3), which becomes red-shifted as the radius increases. We found that a radius of 6 Å is optimal for this particular problem, which gives 40 movable zeolite atoms, as shown in Fig. 2.

Here we describe our standard implementation of normal-mode analysis. For simplicity, the analysis below explicitly includes only the N movable zeolite atoms. However, each forcefield calculation performed to parametrize normal-mode analysis includes contributions from all 576 atoms under periodic boundary conditions, regardless of the number of atoms allowed to move. The configuration of N movable atoms in three dimensions is denoted by the $3N$-dimensional vector $\vec{\mathbf{r}}^N = (\vec{\mathbf{r}}_1, \vec{\mathbf{r}}_2, \vec{\mathbf{r}}_3, \ldots, \vec{\mathbf{r}}_N)$, where $\vec{\mathbf{r}}_i$ is the three-dimensional Cartesian position of atom i. Likewise, the ground-state configuration is denoted by $\vec{\mathbf{r}}_0^N = (\vec{\mathbf{r}}_1^{(0)}, \vec{\mathbf{r}}_2^{(0)}, \vec{\mathbf{r}}_3^{(0)}, \ldots, \vec{\mathbf{r}}_N^{(0)})$. We denote a displacement from the ground state by $\Delta\vec{\mathbf{r}}^N = \vec{\mathbf{r}}^N - \vec{\mathbf{r}}_0^N = (\Delta\vec{\mathbf{r}}_1, \Delta\vec{\mathbf{r}}_2, \Delta\vec{\mathbf{r}}_3, \ldots, \Delta\vec{\mathbf{r}}_N)$. Finally, the mass-weighted displacement is $\Delta\vec{\mathbf{s}}^N = (\sqrt{m_1}\Delta\vec{\mathbf{r}}_1, \sqrt{m_2}\Delta\vec{\mathbf{r}}_2, \sqrt{m_3}\Delta\vec{\mathbf{r}}_3, \ldots, \sqrt{m_N}\Delta\vec{\mathbf{r}}_N)$. Given these definitions, the harmonic approximation for the zeolite potential energy is given by

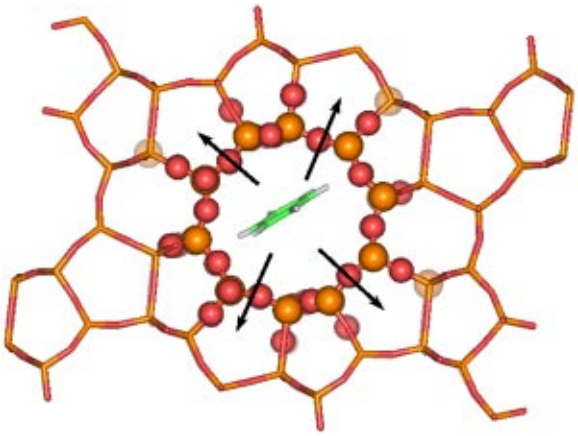

FIG. 2. Benzene (center) in the straight channel of silicalite. The highlighted framework atoms produce channel breathing, and are included in "local normal-mode" analysis.

$$V_Z(\vec{\mathbf{r}}^N) \cong V_Z(\vec{\mathbf{r}}_0^N) + \frac{1}{2}\sum_{i=1}^{N}\sum_{j=1}^{N} \Delta\vec{\mathbf{r}}_i \cdot \left(\frac{\partial^2 V_Z}{\partial\vec{\mathbf{r}}_i \partial\vec{\mathbf{r}}_j}\right)_0 \cdot \Delta\vec{\mathbf{r}}_j, \quad (3)$$

$$= V_Z(\vec{\mathbf{r}}_0^N) + \frac{1}{2}\sum_{i=1}^{N}\sum_{j=1}^{N} \Delta\vec{\mathbf{s}}_i \times \left[\frac{1}{\sqrt{m_i}}\left(\frac{\partial^2 V_Z}{\partial\vec{\mathbf{r}}_i \partial\vec{\mathbf{r}}_j}\right)_0 \frac{1}{\sqrt{m_j}}\right] \cdot \Delta\vec{\mathbf{s}}_j, \quad (4)$$

where $(\partial^2 V_Z / \partial\vec{\mathbf{r}}_i \partial\vec{\mathbf{r}}_j)_0$ is a 3×3 force constant matrix evaluated at the ground-state zeolite geometry. We evaluate these second derivatives by first calculating first derivatives analytically using the standard force routines in our program DIZZY.[31] We then compute second derivatives using two-point, symmetric finite differences of the forces along *x*-, *y*-, and *z*-directions for each pair of movable atoms in the system. We have found that a grid spacing of 10^{-4} Å gives robust convergence of these second derivatives.

In Eq. (4), the quantity in $[\cdots]$ is the "mass-weighted" force constant matrix, which is the central object in normal-mode analysis. We diagonalize this matrix using standard direct methods, such as the Householder method,[32] whose memory and time requirements scale as N^2 and N^3, respectively. The diagonalization routine outputs the $3N$ eigenvalues and eigenvectors of the mass-weighted force constant matrix. The eigenvalues (k_i) have units of force constant/mass which yields the square of the vibrational frequency: $k_i = \omega_i^2 = (2\pi c \bar{\nu}_i)^2$, where c is the speed of light and $\bar{\nu}_i$ is the vibrational wave number of the ith normal mode, typically reported in cm^{-1}. The eigenvectors ($\vec{\mathbf{U}}_i$) are automatically orthonormal, i.e., $\vec{\mathbf{U}}_i \cdot \vec{\mathbf{U}}_j = \delta_{ij}$. In terms of these eigenvectors, the normal-mode vibrational coordinates (Q_i) are expressed as

$$Q_i = \sum_{j=1}^{3N} (\vec{\mathbf{U}}_i)_j (\Delta \vec{\mathbf{s}}^N)_j . \tag{5}$$

In terms of these coordinates, the harmonic potential energy simplifies to

$$V_Z(\vec{\mathbf{Q}}) \cong V_Z(\vec{\mathbf{0}}) + \tfrac{1}{2} \sum_{j=1}^{3N} k_i Q_i^2 . \tag{6}$$

To calculate zeolite–guest potential energies, which are evaluated using Cartesian coordinates, we need the inverse normal-mode transformation given by

$$(\Delta \vec{\mathbf{s}}^N)_j = \sum_{i=1}^{3N} (\vec{\mathbf{U}}_i)_j Q_i . \tag{7}$$

Equation (7) follows from the orthonormality of the eigenvectors $\vec{\mathbf{U}}_i$.

We have now introduced the quantities required to summarize our local normal-mode Monte Carlo algorithm. Here we describe its application for calculating the average Metropolis acceptance probability to jump from slice A to B, i.e., $\langle M_\beta(\Delta V)\rangle_A$ in Eq. (2). First we compute and diagonalize the mass-weighted force constant matrix; obviously this step is performed once only. Next we initialize the zeolite at $\vec{\mathbf{r}}^N_{\text{old}} \leftrightarrow \vec{\mathbf{Q}}_{\text{old}}$ and the guest in slice A; $\vec{\mathbf{r}}^N_{\text{old}}$ can be $\vec{\mathbf{r}}^N_0$ or some equilibrium configuration from a previous Monte Carlo simulation. We then use our forcefield to compute the initial zeolite–guest potential, $V_{ZG}(\text{old})$, and we use Eq. (6) to compute the initial zeolite potential energy, $V_Z(\text{old})$.

A guest jump is then chosen at random, either a real move within slice A, or a fictitious jump from A to B using the displacement-vector distribution described above. Next we create a zeolite distortion by randomly choosing a normal mode $i \in [1,3N]$ and a length $\lambda \in [-\lambda_{\max}, \lambda_{\max}]$, where $\lambda_{\max} = 2\ \text{Å}(N/576)$ was found to give efficient Monte Carlo sampling of lattice vibrations for various values of N. Following Eq. (7), the mass-weighted Cartesian displacement vector is updated according to

$$\Delta \vec{\mathbf{s}}^N_{\text{new}} = \Delta \vec{\mathbf{s}}^N_{\text{old}} + \lambda \vec{\mathbf{U}}_i . \tag{8}$$

The new (un-mass-weighted) zeolite configuration, $\vec{\mathbf{r}}^N_{\text{new}}$, is trivially obtained from $\Delta \vec{\mathbf{s}}^N_{\text{new}}$, allowing forcefield evaluation of the new zeolite–guest potential, $V_{ZG}(\text{new})$. The zeolite potential is updated according to:

$$V_Z(\text{new}) = V_Z(\text{old}) + \tfrac{1}{2}[(Q_i + \lambda)^2 - Q_i^2], \tag{9}$$

where Q_i is the ith element of $\vec{\mathbf{Q}}_{\text{old}}$. We thus keep track of zeolite configurations in both Cartesian and normal-mode coordinates. The total potential energy change, $\Delta V = \Delta V_Z + \Delta V_{ZG}$, is then fed into the Metropolis function $\langle M_\beta(\Delta V)\rangle_A$ for determining whether to accept the move. If the move is accepted, then Q_i is replaced with $Q_i + \lambda$, all "new" labels are replaced with "old," and so forth millions of times.

Here we give some timings characteristic of our algorithm applied to benzene in silicalite. On a 1.7 GHz Xeon processor, DIZZY requires about 0.08 CPU seconds with 40 movable zeolite atoms and 0.6 CPU seconds with 576 movable atoms to calculate the zeolite potential using a standard forcefield. On the other hand, using our local normal-mode approach, DIZZY requires just 0.005 CPU seconds per evaluation, independent of the number of movable atoms. This efficiency comes at a small cost—the zeolite normal modes must be calculated and stored once at the start of the simulation. The computational expense of this step, which depends on the the number of movable atoms, is about 10 CPU seconds for 40 atoms and about 23 minutes for 576 atoms. The cost of calculating normal modes is found to be a tiny fraction of the total CPU time required for converging the FES. Thus, our flexible-lattice algorithm is as efficient, step for step, as a fixed-lattice one. What's more, the flexible-lattice FES calculations below converged in fewer Monte Carlo steps than did the fixed-lattice ones, because of the increased likelihood of jumping through a flexible lattice.

III. RESULTS AND DISCUSSION

We describe the results of normal-mode calculations on bare silicalite, and on silicalite with benzene adsorbed in the straight channel, to gauge the accuracy of the harmonic approximation. We then discuss free energy calculations for benzene in fixed and flexible silicalite, to determine the efficiency of the new algorithm.

A. Testing the harmonic approximation

There are various manifestations of harmonic behavior that can be used to test the accuracy of this approximation for estimating zeolite distortion energies. We use the following two:

(1) Spectrum of normal-mode wave numbers is independent of configuration;

(2) potential energy, averaged in the canonical ensemble, is linear in temperature.

Any deviation from these properties signals the importance of anharmonicity. To explore criterion (1), we ran MD simulations at 300 K on bare silicalite, and on silicalite with benzene adsorbed in the straight channel. From both these simulations, we extracted lattice configurations at 10, 20, 30, and 40 ps, totaling eight distinct zeolite configurations. The configurations extracted from MD with benzene strain the lattice because of benzene's tight fit in silicalite's straight channel. For each of these configurations we calculated the full set of 1728 normal-mode wave numbers; these wave numbers were then histogrammed using a bin width of 30 cm^{-1}. The resulting histograms are shown in Fig. 3. All eight histograms in Fig. 3 are essentially identical. Each histogram shows a Debye region for $\bar{\nu} < 100\ \text{cm}^{-1}$, roughly five overlapping bands for $100\ \text{cm}^{-1} < \bar{\nu} < 1000\ \text{cm}^{-1}$, and two clear overlapping bands for $1000\ \text{cm}^{-1} < \bar{\nu} < 1350\ \text{cm}^{-1}$. The fact that this histogram shape is conserved when loading benzene into silicalite's straight channel lends much credence to the harmonic approximation advocated herein.

To explore criterion (2), we performed MD on bare silicalite at temperatures of 100–600 K, using our Coulomb–Buckingham forcefield. During these simulations, we averaged the potential energy of distorting silicalite, i.e., we computed $\langle V_Z - V_Z(\vec{\mathbf{r}}^N_0)\rangle_{NVT}$. For comparison, we computed

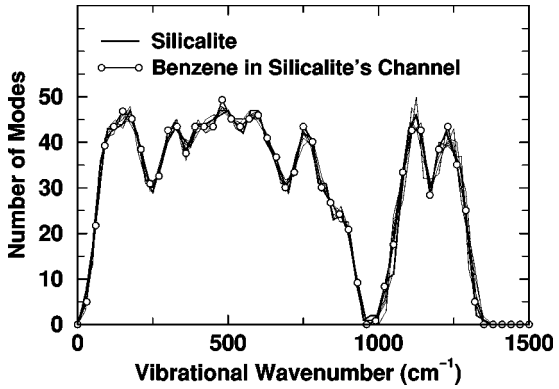

FIG. 3. Histograms of normal-mode wave numbers for silicalite: four histograms constructed from normal-mode analysis applied to silicalite structures extracted at 10, 20, 30, and 40 ps of 300 K molecular dynamics of bare silicalite (lines); 4 more histograms obtained in the same way, except with benzene in silicalite's straight channel (dots).

the same quantity using Metropolis Monte Carlo implemented with harmonic distortion energies. These results are shown in Fig. 4. The average distortion energy obtained from the forcefield is essentially identical to the harmonic Monte Carlo result, both linear with temperature. Also plotted is the harmonic result from classical statistical mechanics: $\frac{3}{2}Nk_BT$, which agrees very well with both MD and Monte Carlo. The differences from MD at 600 K are only about 1%. These results lend further credence to the notion of making a harmonic approximation to zeolite distortion energies.

B. Benzene free energies in silicalite

The free energy landscape for benzene in silicalite is now reasonably well known,[8,22] with relatively flat minima at intersection sites and corrugated regions of high free energy in channels. This landscape arises from a balance between the host-guest potential energy, host distortion energy and guest configurational entropy. Using the methods outlined above, we calculated benzene's FES along the crystallographic *y*-axis describing the jump between intersection sites, which are separated by about 10 Å. In Fig. 5 we compare results for flexible and rigid lattices. Both curves show the qualitative features indicated above. However, the rigid-lattice barrier is much higher than the flexible-lattice one, because the zeolite is allowed to distort during the latter simulations. Our flexible-lattice FES is in excellent agreement with results of Forester and Smith.[8] In agreement with their results, we find three shallow free-energy minima in the channel. Our barrier, 20 kJ mol^{-1}, is in very good agreement with their result, 25 kJ mol^{-1}, considering that slightly different forcefields were used. These results confirm that our local normal-mode Monte Carlo approach can faithfully represent molecular motion in tight-fitting zeolite–guest systems.

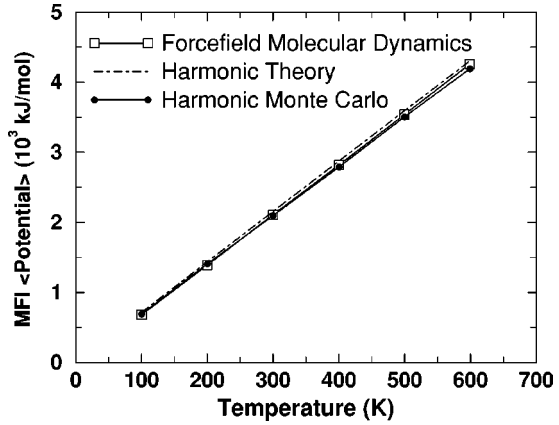

FIG. 4. Average potential energy of silicalite vs temperature for all 576 zeolite atoms, relative to the ground-state potential energy. Computed from forcefield-based molecular dyanmics (squares), normal-mode Monte Carlo (dots), and harmonic statistical mechanics (dashed line).

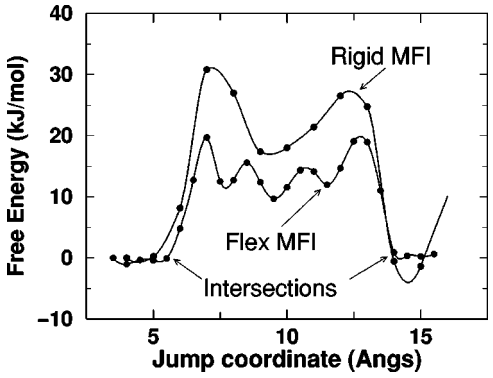

FIG. 5. Free energy surfaces for benzene motion through silicalite's straight channel, from one intersection to the next. Results from flexible and rigid frameworks are compared.

For each flexible-lattice free energy in Fig. 5, we performed two Monte Carlo runs of length 10^6 steps (attempted moves). On the other hand, for each rigid-lattice free energy we performed two Monte Carlo runs of length 9×10^6 steps. We note that the rigid-lattice FES does not reflect silicalite's symmetry along the reaction coordinate, while the flexible-lattice FES does. This indicates that, despite the longer Monte Carlo runs, the rigid-lattice FES remains more poorly converged than the flexible-lattice FES. This slow convergence occurs because of the decreased likelihood of jumping through a rigid lattice. A more efficient window sampling method might speed up the rigid-lattice FES convergence.[33] Nonetheless, because the normal-mode algorithm makes rigid- and flexible-lattice calculations equally fast step for step, and our flexible calculations converged in fewer steps, we have shown that flexible-lattice calculations can actually be *faster* than rigid-lattice ones.

IV. SUMMARY AND CONCLUDING REMARKS

We have developed and applied an efficient Monte Carlo algorithm for simulating diffusion in tight-fitting host–guest systems, based on using zeolite normal modes. We gained computational efficiency by sampling framework distortions using normal-mode coordinates, and by exploiting the fact that zeolite distortion energies are well approximated by harmonic estimates. We obtained additional savings by performing local normal-mode analysis, i.e., only including the motions of zeolite atoms close to the jumping molecule, hence focusing the calculation on zeolite distortions relevant to

guest diffusion. We performed normal-mode analysis on various silicalite structures to demonstrate the accuracy of the harmonic approximation. We computed free energy surfaces for benzene in silicalite, finding excellent agreement with previous theoretical studies. Our method was found to be orders-of-magnitude faster than comparable Monte Carlo calculations that use conventional forcefields to quantify zeolite distortion energies. For tight-fitting guests, the efficiency of our new method allows flexible-lattice simulations to converge in less CPU time than that required for fixed-lattice simulations, because of the increased likelihood of jumping through a flexible lattice.

This algorithm will facilitate simulations of adsorption and diffusion in tight-fitting host–guest systems for hosts that behave as multidimensional harmonic oscillators during guest diffusion. This class of hosts includes most siliceous zeolites, many carbon nanotubes, and possibly the selectivity filters of biological ion channels. Exceptions include zeolites that undergo phase transitions upon guest adsorption, zeolites with exchangeable cations that diffuse alongside guests, biological ion pumps, and any host that executes large amplitude motion during guest diffusion.

A possible solution for modeling guest diffusion in cation-containing zeolites is to partition the system into harmonic and anharmonic degrees of freedom. The aluminosilicate framework remains largely harmonic, while the guest and cation motions are rather anharmonic. Our local normal-mode Monte Carlo algorithm provides significant speed-ups only if the number of harmonic coordinates greatly exceeds the number of anharmonic ones. In the future we plan to apply this approach to model diffusion of guests that fit tightly in cation-containing zeolites, to gauge the method's efficiency under these more demanding circumstances.

ACKNOWLEDGMENTS

One of the authors (S.C.T.) acknowledges undergraduate research fellowships from the Commonwealth College of the University of Massachusetts at Amherst, and from Microsoft, Inc. The authors acknowledge generous funding from the National Science Foundation CAREER Program (NSF CTS-9734153), and from the UMass Amherst Department of Chemistry for computational resources. S.M.A. is a Sloan Foundation Fellow and a Camille Dreyfus Teacher-Scholar.

[1] J. Kärger and D. M. Ruthven, *Diffusion in Zeolites and Other Microporous Solids* (Wiley, New York, 1992).
[2] N. Y. Chen, T. F. Degnan, Jr., and C. M. Smith, *Molecular Transport and Reaction in Zeolites* (VCH, New York, 1994).
[3] H. van Koningsveld, F. Tuinstra, H. van Bekkum, and J. C. Jansen, Acta Crystallogr. Sect. B Struct. Commun. **45**, 423 (1989).
[4] B. F. Mentzen and P. Gelin, Mater. Res. Bull. **30**, 373 (1995).
[5] B. F. Mentzen and F. Lefebvre, Mater. Res. Bull. **32**, 813 (1997).
[6] G. Xomeritakis and M. Tsapatsis, Chem. Mater. **11**, 875 (1999).
[7] H. Karsh, A. Culfaz, and H. Yucel, Zeolites **12**, 728 (1992).
[8] T. R. Forester and W. Smith, J. Chem. Soc., Faraday Trans. **93**, 3249 (1997).
[9] P. Demontis, E. S. Fois, and G. B. Suffritti, and S. Quartieri, J. Phys. Chem. **94**, 4329 (1990).
[10] C. R. A. Catlow, C. M. Freeman, B. Vessal, S. M. Tomlinson, and M. Leslie, J. Chem. Soc., Faraday Trans. **87**, 1947 (1991).
[11] P. Demontis, G. B. Suffritti, E. S. Fois, and S. Quartieri, J. Phys. Chem. **96**, 1482 (1992).
[12] K. S. Smirnov, Chem. Phys. Lett. **229**, 250 (1994).
[13] A. Bouyermaouen and A. Bellemans, J. Chem. Phys. **108**, 2170 (1998).
[14] S. Fritzsche, M. Wolfsberg, R. Haberlandt, P. Demontis, G. P. Suffritti, and A. Tilocca, Chem. Phys. Lett. **296**, 253 (1998).
[15] P. Santikary and S. Yashonath, J. Phys. Chem. **98**, 9252 (1994).
[16] G. Schrimpf, M. Schlenkrich, J. Brickmann, and P. Bopp, J. Phys. Chem. **96**, 7404 (1992).
[17] G. Sastre, C. R. A. Catlow, and A. Corma, J. Phys. Chem. B **103**, 5187 (1999).
[18] T. Mosell, G. Schrimpf, and J. Brickmann, J. Phys. Chem. B **101**, 9476 (1997).
[19] T. Mosell, G. Schrimpf, and J. Brickmann, J. Phys. Chem. B **101**, 9485 (1997).
[20] F. Jousse, D. P. Vercauteren, and S. M. Auerbach, J. Phys. Chem. B **104**, 8768 (2000).
[21] K. T. Thomson, A. V. McCormick, and H. T. Davis, J. Chem. Phys. **112**, 3345 (2000).
[22] R. Q. Snurr, A. T. Bell, and D. N. Theodorou, J. Phys. Chem. **98**, 11948 (1994).
[23] K. A. Iyer and S. J. Singer, J. Phys. Chem. **98**, 12 679 (1994).
[24] C. Blanco and S. M. Auerbach, J. Am. Chem. Soc. **124**, 6250 (2002).
[25] C. Blanco and S. M. Auerbach, J. Phys. Chem. B (to be published).
[26] C. Baerlocher, W. M. Meier, and D. H. Olson, *Atlas of Zeolite Framework Types*, 5th ed. (Elsevier, Amsterdam, 2001) (http://www.iza-structure.org/databases).
[27] E. Jaramillo and S. M. Auerbach, J. Phys. Chem. B **103**, 9589 (1999).
[28] S. M. Auerbach, N. J. Henson, A. K. Cheetham, and H. I. Metiu, J. Phys. Chem. **99**, 10 600 (1995).
[29] F. Jousse and S. M. Auerbach, J. Chem. Phys. **107**, 9629 (1997).
[30] A. Voter, J. Chem. Phys. **82**, 1890 (1985).
[31] N. J. Henson, S. M. Auerbach, and B. K. Peterson, DIZZY: Dynamics in Zeolites (1999).
[32] W. H. Press, S. A. Teukolsky, W. T. Vetterling, and B. P. Flannery, 2nd ed. *Numerical Recipes in Fortran 77: The Art of Scientific Computing* (Cambridge University Press, New York, 1992).
[33] D. Frenkel and B. Smit, *Understanding Molecular Simulations* (Academic, San Diego, 1996).